

MIE 415 Final Report

1411

Guide Dog Robot

Sponsored by: Dynamic and Autonomous Robotic Systems Lab, UMass Amherst

December 6th, 2024

Ken Suzuki	- Team Lead
Shaylyn Tavaréz	- Analysis Lead
Salani Seneviratne	- Design Lead
Connor Delaney	- Fabrication Lead
Georges Chebly	- Controls/Electrical Lead
Peter White	- Evaluation Lead

Executive Summary

For the past three years, the Dynamic and Autonomous Robotic Systems (DARoS) Laboratory at UMass Amherst has been conducting studies on guide dog robots. However, the lab's current research platform, the commercially available UniTree Go1 quadruped robot, lacks the ability to climb stairs. Although the DARoS Lab has explored other commercial quadruped robots, none offer both good portability and stair-climbing capabilities at the same time. To address this gap, we present Vivo, our attempt at creating a prototype quadruped robot that offers both stair-climbing capabilities and portability by being able to fit within standard carry-on luggage dimensions. Vivo's legs are designed to closely mimic dog legs, which have been long proven to be effective at stair climbing. The leg lengths are also optimized for stair climbing based on kinematic analysis. Additionally, the robot collapses to smaller than carry-on luggage dimensions, making it portable for daily use.

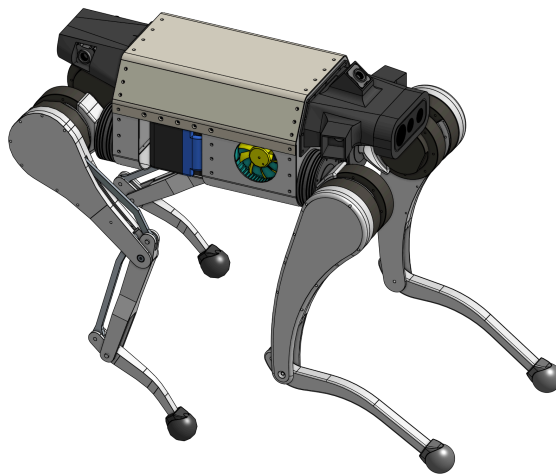


Figure 1. Final Design of Robot Guide Dog

Summary of Impact

The sponsors of this project sought to develop cutting-edge software for quadruped robots with the goal of creating a robot guide dog. While they have made progress towards achieving this goal, the hardware currently used for testing has proved to be the limiting factor in their research. For this reason our team has developed a prototype quadruped robot specifically designed to function as a guide dog. By addressing key issues faced by our sponsor such as stair climbing ability and portability we lay the groundwork for the lab's future research into robot guide dogs. This prototype will help establish the foundation for testing the concept of a specialized quadruped guide dog robot, effectively acting as a prototype for future versions. In the future this research will have been the first step towards the creation of a fully fledged robotic mobility aid for blind and low-vision (BLV) individuals.

Introduction and Objectives

Introduction

Guide dogs are a popular aid for BLV individuals as they provide the user with greater mobility, confidence, and independence. However, guide dogs have several drawbacks that make them unsuitable for some people. A new guide dog generally requires two or more years of training before they are capable of working effectively, which can cost over \$40,000. Along with the upfront cost, dogs cost approximately \$1,200 yearly for general care ("How Much Does A Guide Dog Cost?"). Additionally, owning a dog comes with a lot of responsibility: they need consistent grooming, veterinary visits, and regular exercise. Finally, guide dogs typically work for only eight years, at which point the owner may have formed a strong bond, making it emotionally challenging to transition to a new dog (Hwang). In contrast, a robot guide dog offers a lower barrier of entry for BLV individuals seeking a reliable mobility aid. Unlike traditional guide dogs, a robot guide dog could be purchased off-the-shelf without a waitlist or need for extensive training. Both the upfront and annual cost of a robot guide dog would be cheaper than that of a traditional guide dog, providing a more affordable and sustainable solution.

Objectives

The main objective of our project is to design and fabricate the body and legs of a power-efficient, lightweight quadruped robot guide specialized for blind and low-vision individuals, by offering legs capable of achieving stair climbing while ensuring a compact body for portability and user-friendliness. The DARoS lab has been using the Unitree Go 1 robot to explore computer vision applications for guide dog assistance, but significant hardware limitations—including short battery life

(~15 minutes), inability to climb stairs, a narrow field of view, and hind leg interference—restrict its usability for blind and low-vision (BLV) individuals. Vivo is designed to address all these issues and offer chances for better computer vision studies.

Related Works

The use of robotic systems as a mobility aid for BLV individuals have been investigated as early as 1976, starting with the MELDOG project, in the shape of a wheeled robot (Tachi). Since then, robotic mobility aids have taken the shape of drones (Al Zavier), smart canes (Slade), and advanced wheeled robots (Guerreiro).

In recent years, the locomotion of quadruped robots have become robust enough for commercial use and have become an increasingly popular solution to automating undesirable tasks, such as safety inspection (“Industrial Inspection Solutions”). One of the underlying benefits of quadruped robots is their ability to traverse urban environments effectively, which makes them an attractive solution to mobility assistance for blind and low-vision individuals (Hwang).

Based on extensive qualitative research with guide dog users conducted by our sponsor, Hwang et. al, we aim to tackle the current limitations of portable quadruped robots for use as a mobility aid (Hwang). Currently, no commercially available quadruped robot matches the portability and stair-navigation abilities of a guide dog. Larger scale quadrupeds like the Boston Dynamics Spot robot and ANYbotics ANYmal C excel in stair-climbing, but their size makes them impractical for portable use. On the other hand, medium to small-scale robots such as the Unitree Go generation robots offer portability but lack the capability to traverse stairs of normal height (17.78 x 27.94 cm per ADA standards), which is required for a guide dog robot. This limitation creates a need for a compact quadruped robot that can traverse stairs (“Chapter 5: Stairways”).

With proper training, guide dogs have excellent street traversing capabilities and can climb stairs effortlessly (“Guide Dog Class Lectures: Working in Buildings”). This skill can be partly attributed to the anatomy of dog legs, which have been optimized for increased efficiency as a result of thousands of years of evolution. Inspired by the kinematics of legged animals, many quadruped robot designs incorporate bio-inspired mechanisms (Seok). Studies have shown that bio-inspired leg designs composed of redundantly actuated parallel mechanisms lead to higher efficiency in ground reaction force generation while also lowering power consumption, which is beneficial for both locomotion tasks and prolonging battery life (De Vicenti; Lee). Despite these advantages, a large number of commercially available quadruped robots today use a simpler two link, non-redundant leg design, which reduces mechanical complexity, but in turn sacrifices efficiency (De Vicenti; “Unitree Go1”). To

satisfy customer requirements for stair climbing, our leg design takes inspiration from the anatomy of dog legs.

Contributions of Each Team Member

Table 1. Team Member Contributions and Project Impact

Team Member/Role	Contributions
Ken Suzuki Team Lead	<ul style="list-style-type: none"> Modeled initial concept in OnShape (body and legs) Communicated with team sponsors regarding progress, analysis, and design choices Conducted kinematic and inverse dynamics analysis of leg designs
Shaylyn Tavaréz Analysis Lead	<ul style="list-style-type: none"> Conducted structural by-hand analysis of robot legs Led Presentation for faculty analysis review Created shear force and moment diagrams for links Determined key design constraints Researched methods to perform structural analysis of robot
Salani Seneviratne Design Lead	<ul style="list-style-type: none"> Researched methods to perform structural analysis of robot Performed structural by-hand analysis on the robot's leg designs under two conditions: <ul style="list-style-type: none"> Equilibrium state Maximum dynamic load Communicated with faculty for analysis review Conducted calculations to find the impact forces on the robot
Connor Delaney Fabrication Lead	<ul style="list-style-type: none"> Performed FEA analysis of leg assembly Assisted team lead with statics analysis Assisted controls lead with interior configuration of robot Modified designs with the goal of improving manufacturability Writing for reports and AOIs
Georges Chebly Controls/Electrical Lead	<ul style="list-style-type: none"> Optimized the body shape to make it manufacturable, compact, and able to fit within carry-on suitcase dimensions

	<ul style="list-style-type: none"> • Helped team lead in the inverse dynamics analysis • Worked on the interior of the robot <ul style="list-style-type: none"> ○ Decided on the electronics configuration ○ Designed mounts for electronics (cameras, computers...)
Peter White Evaluation Lead	<ul style="list-style-type: none"> • Helped with the preliminary and necessary research throughout the semester including material standards for Aluminum 6061-T6 and 1018 Carbon Steel, stair climbing and mobility analysis, and batteries • Helped prepare for all AOIs, and write reports • Presented the House of Quality and part of the PRP • Performed ANSYS analysis on the shank of the robot leg (ended up not using ANSYS) • Will be working on PCB design during break

Functional Decomposition

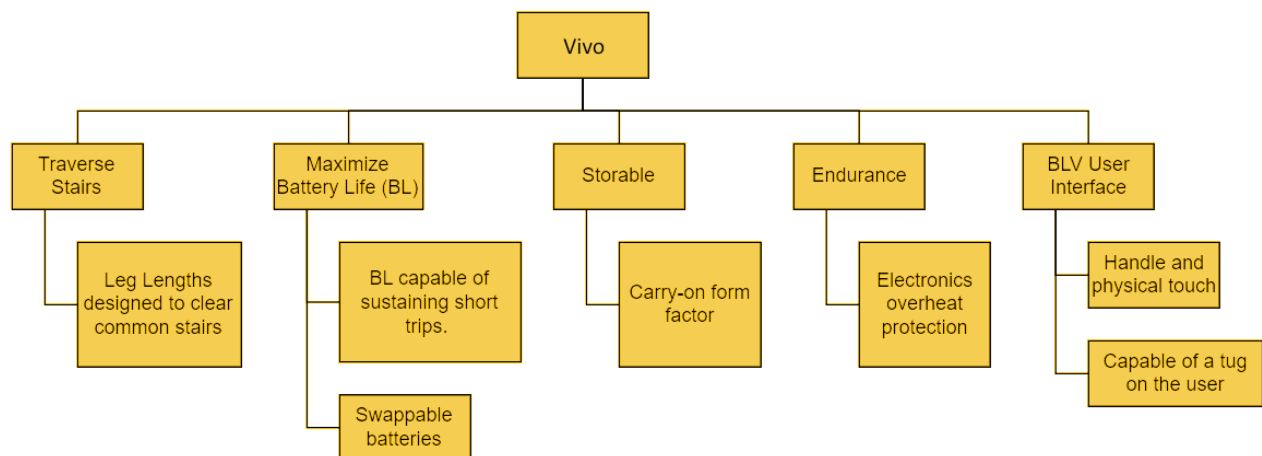


Figure 2. Functional Decomposition of Our Robot

In order to create a guide dog robot that meets the needs of a BLV user, the robot should be capable of performing five key functions, as illustrated in Fig. 2. First, the robot should be able to

navigate urban terrain, which is crucial for guiding users during their travels. This includes overcoming common obstacles, such as stairs. To address this challenge the robot must have leg lengths and geometry capable of combating such obstacles. Second, the robot needs sufficient power to support typical outings, like trips to the grocery store. This means the product needs to be designed to maximize battery life, to keep up the robot's endurance for long trips, the electronic components need protection from overheating. For everyday travel, BLV users often use public transportation. For these experiences to go smoothly, the user must be able to store and carry the robot with relative ease. The last key function a robot dog must achieve is a user interface. The dog will require some sort of handle, physical touch features, and the ability to tug the user in the direction of travel.

Engineering Standards and Patents

Material Standards

The final design analysis was done using two material standards. The majority of the robot is made up of aluminum 6061-T6 and the transmission link is made of 1018 carbon steel. The ASTM standard specification for aluminum 6061-T6 material strength was used in analysis and the AISI/SAE 1018 carbon steel specification is set to be used in future analysis for steel components. The ASTM standard specifies aluminum 6061-T6 to have an ultimate tensile strength (UTS) of 260 MPa and yield strength (YS) of 240 MPa. The AISI/SAE mechanical properties for 1018 carbon steel are rated at a UTS of 440MPa and a YS of 370MPa. These standards help to improve the quality of our design by providing reliable material properties for analysis.

Robotics Standards

ISO 13482 sets guidelines for the safety of personal care robots with respect to electrical, mechanical, and software aspects. These guidelines have helped pave the design process to ensure maximal safety and reliability. Following the guidelines for robot design, hard stop limits at each joint for singularity protection must be incorporated. Joints shall not be capable of crushing any body parts. User interface guidelines highlight the need for status indication and avoidance of sharp edges and points on the robot.

Manufacturing Standards

ISO 286 provides guidelines for tolerancing components in 2D drawings. As our sponsor intends to fund the manufacturing of robot parts through an overseas contract manufacturer, this standard will serve as the basis for communicating the geometry and tolerances of our components to them. This will be crucial for reliable operation of the legs.

Stair Standards

ADA § 504 & IRC § R311.7 outline the requirements for both residential and commercial staircases, including the maximum and minimum lengths for stair steps (“Chapter 5: Stairways”). Designing our robot to be capable of climbing stairs means it must be able to climb the tallest stairs as specified by these codes to ensure compliance with standards. According to the International Code Council, the maximum step height is twenty centimeters and the minimum step length is twenty-five centimeters (International Residential Code). In contrast, the Americans with Disabilities Act defines the maximum step height as eighteen centimeters and the minimum step length is twenty-eight centimeters.

Patents

Patents were used to gain knowledge of the current competition and to obtain inspiration for our robot design. Boston Dynamics’ Spot robot features an elbow joint actuated by a ball screw mechanism acting as a prismatic joint, which differs from belt driven or parallel link driven mechanisms that are popular in small scale quadruped robots (Potter). Although this mechanism is complex compared to other elbow actuation methods, it is highly efficient at transmitting force. The ANYmal C robot developed by ANYbotics features a limb between its top and bottom links, with a built-in Series Elastic Actuator that introduces passive compliance into the joint, which is a feature not present in traditional planetary gear box reduced brushless DC motor actuators (Scafato).

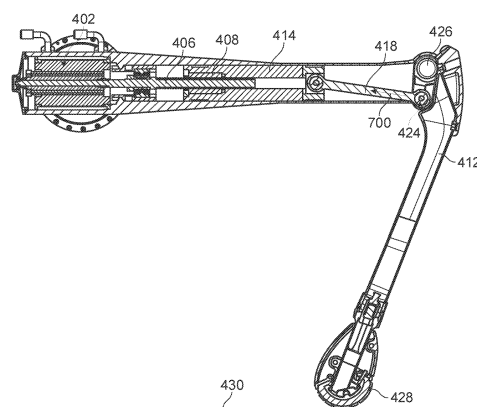


Figure 3. Leg design of Boston Dynamics’ Spot robot (Potter).

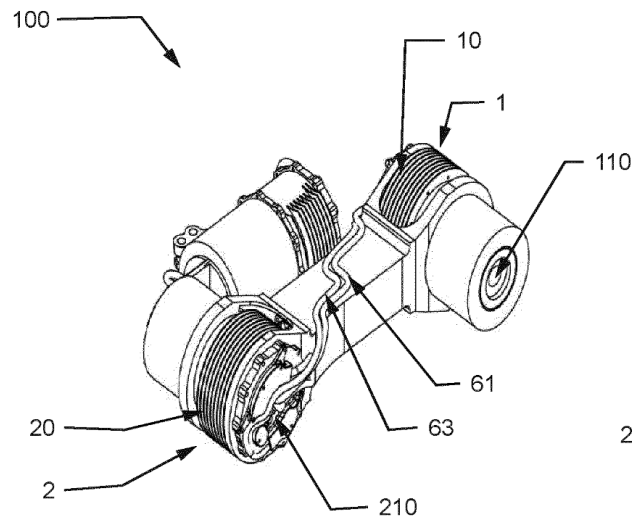


Figure 4. Limb design with incorporated series elastic actuators, developed by ANYbotics (Scafato).

Specifications

Table 2. Customer Requirements

Requirement	Weight (Importance: 1 (Least) → 6 (Most))
Storability/Small Size	4
Temperature Control	2
Operating Time	5
Portability	3
Cost	1
Hardware For Stair Climbing	6

The customer presented an initial list of requirements at the start of the semester which was refined through communication with the sponsor over the first month. The customer expressed that the final product must meet three major requirements: hardware cable of stair climbing, good battery life, and a portable form factor. From this, the team made these requirements of utmost importance

as seen in Table 3. The requirement of a portable form factor is split into storability and portability since the customer emphasized that the quadruped should be lightweight, and be able to fold into airplane carry-on luggage size. In order for the robot to run effectively without overheating issues, temperature control was a must and was later decided as a customer requirement. Cost was put low on the list since the customer is open to financing the final product if the requirements are met, but the budget as with any project is still a consideration.

Table 3. Target Engineering Specifications

	Reachable Workspace (rise/go) [m/m]	Battery Capacity [Wh]	Mass [kg]	Storage Volume [m³]	Operating Temperature [C°]
Ideal Values	0.20/0.25	288	≤ 21.5	< 0.45	< 55
Marginal Values	0.18/0.28	134	25	0.45	55

The engineering requirement specifications are presented in Table 2. The storage volume criterion was determined by using the average maximum collapsible carry-on volume in the United States of $55.88 \times 35.56 \times 22.86 \text{ cm}^3$. Achieving this form factor is necessary, but any value below this is ideal (Norcross). The operating temperature was determined as the maximum temperature the internal computers could withstand based on their respective data sheets. An ideal weight of 21.5 kg was imposed based on the weight of the Unitree Aliengo robot, which is slightly larger in size than our maximum allowable dimensions. The customer wanted a robot dog that has higher endurance than their previous robot, the Unitree Go1 which has a rating of 133Wh, so the marginal target is slightly above this value at 134Wh. The ideal value is an estimated maximum value of 288Wh, equivalent to a 0.76 hour battery life based on our proposed battery setup (Appendix C). The dog's ability to climb stairs is based on research out of the Italian Institute of Technology, which found that quadrupeds that have successful foot candidate positions that cover at least 20% of the “Go” surface climb stairs effectively. In accordance with the previously discussed IRC § R311.7 and ADA § 504 standards, we determined the ideal and marginal rise/go values that the robot must be able to climb. The ideal value was established using the higher rise/go ratio from the two standards, while the marginal value was based on the lower ratio.

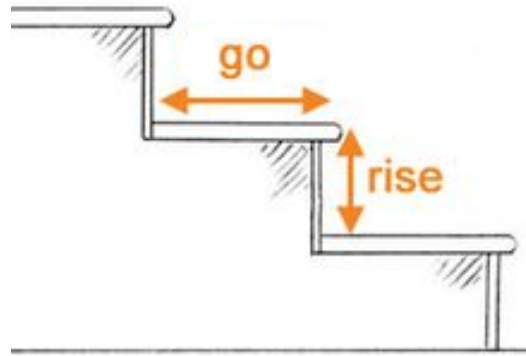


Figure 5. Staircase diagram defining rise and go.

Similar products were compared to further determine the necessities of each customer requirement. As seen in Table 4, our product has the best overall combination of the customer requirements compared to other options on the market. The UniTree Go1, a small-scale quadruped robot, excels in terms of storability and portability; however, it is unable to climb standard stairs. The UniTree Aliengo and Boston Dynamics Spot are both larger scale quadruped robots. This allows them to score well in operating time with larger batteries, and hardware for stair climbing with larger legs. However, since they are larger they fail to meet storability and portability requirements.

Table 4. Customer Requirements- Our Design Versus Competition (Order Note: 1 (Worst) → 5 (Best))

	Our Product	Boston Dynamics Spot	UniTree Go1	UniTree Aliengo
Storability	5	0	5	1
Temperature Control	3	5	3	4
Operating Time	3	3	2	5
Portability	5	1	5	4
Cost	4	1	5	2
Hardware for Stair Climbing	4	5	2	4

Design Selection and Solution

Leg Design

The initial leg design consisted of the conventional, simpler two-link leg (Fig. 6) for design simplicity. However, recent works in the field of control aware robot design suggest that bio-inspired leg designs are more dynamically efficient, leading to less power consumption (De Vicenti, Seok). Thus, our second design iteration utilizes a dog-inspired leg design to maximize system efficiency. We modeled our leg designs similar to that of a golden retriever, which is a common dog breed for guide dogs (Durant, Piper). As illustrated in Fig. 7a, our final concept design features different legs for the front and hind legs. The front leg features a two-link, two-degree-of-freedom leg, while the hind leg features a three-link, two-degree-of-freedom leg.

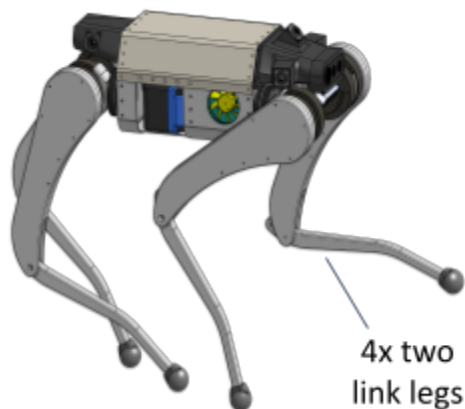


Figure 6. Initial concept of robot with four two link legs.

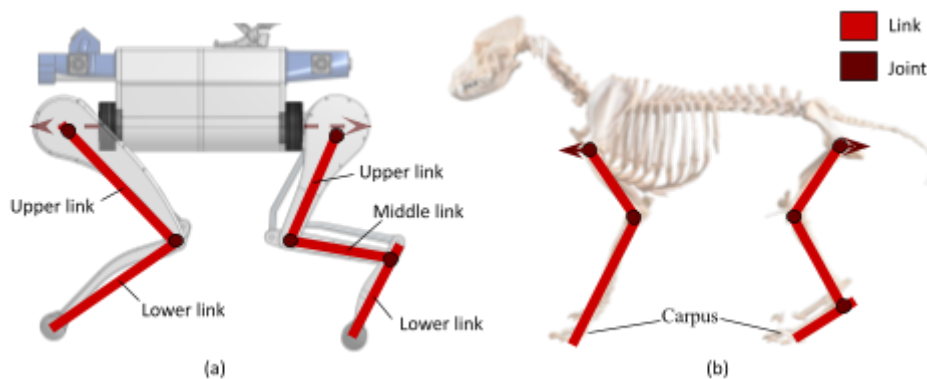


Figure 7. Link configuration of second bio-inspired design iteration. (a) our robot's legs to (b) golden retriever legs (Museum of Veterinary Anatomy FMVZ USP).

Actuation Mechanisms

The leg actuation method was important to decide early on in order to guide our leg design and motor selection. Three systems were considered: transmission links, timing belts, and driving links directly with the motors. Out of these three, the first method to be discarded was driving links directly with the motor. While this system would be the simplest to implement mechanically, it has several drawbacks. Most notably, placing a motor at each joint would increase the mass and thus the inertia of each leg. This results in motors that weigh more, take up more space, consume more power, and cost more. For these reasons driving links directly was discarded.

Timing belts to actuate the legs were the second option considered (Fig. 8b). Compared to directly attaching motors in each joint, timing belts offer several advantages. The moment of inertia in each leg decreases with a timing belt as the weight of the motor is moved into the body of the robot. However, timing belts are hindered by slippage and experience decreased durability when improperly tensioned. If a timing belt is not properly tensioned during use, these issues build up over time leading to premature failure (Layosa). It would be difficult for BLV individuals to perform this maintenance on their own, which motivated the decision to use transmission links (Fig. 8a).

Transmission links have several benefits for a quadruped robot of our size that make them the ideal choice. They allow all the motors in the robot to be located in the body, reducing the moment of inertia in the leg. Transmission links are also very durable which help reduce potential maintenance required in other systems. When the transmission link mechanism is configured in a redundantly actuated, parallel configuration, the elbow joint rotates at the same angle as the motor output angle. This makes the controls of the robot almost as precise as the control of the motor can be. For these reasons, the transmission link was the selected actuation method.

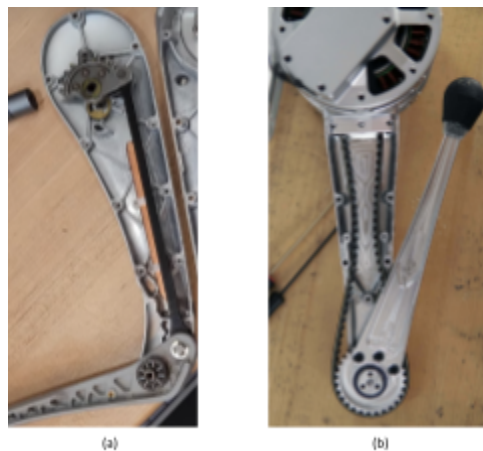


Figure 8. Elbow actuation mechanisms considered.
(a) Transmission link (RegulusRemains) (b) timing belt (Katz).

Motor Selection

Motors were selected based on the dynamic requirements of the robot. Additionally, using lower-power motors was held paramount to prolong the robot's battery life. Since the robot is not intended to perform highly dynamic motions, the motor torque should be able to handle walking and stair climbing and nothing more. Brushless DC motors were selected due to their higher efficiency, lower operating noise, and higher angular velocity compared to other types of motors. They are also the most popular type of actuator used in legged robots today. The selected motors were the T-Motor AK60-6 and T-Motor AK80-9 for the hip roll, and hip pitch and flexion/extension, respectively. Through inverse dynamics calculations, the combined effort of the selected motors are able to withstand approximately twice the robot's estimated weight while standing.

Body Design

The body of the robot will contain all the electronic components to control the robot. It must have the strength to sustain loads from the legs while also being thermally conductive to prevent overheating of the electronics. The outer body will be constructed from aluminum sheets and plates for their high thermal conductivity and lower cost. Compared to other types of materials such as injection molded plastic, aluminum does not require the creation of a custom mold, which would be costly. While 3D printing the body (Fig. 9a) is another option, it may compromise the strength of the structure due to the anisotropic properties of additively manufactured parts. In addition, the thermal conductivity of a plastic is lower relative to most metals, which compromises the heat dissipation. Aluminum was chosen over a metal like copper because of its high strength while also maintaining good thermal conductivity ("Copper, Cu; Annealed").

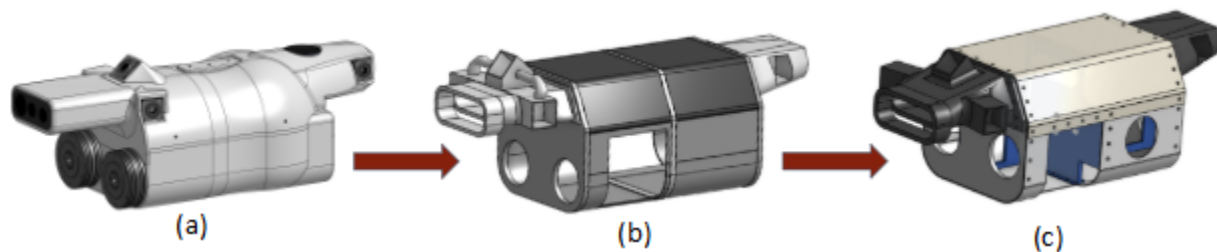


Figure 9. Body design iterations. (a) 3D printed design. (b) Four-piece sheet metal design. (c) Chosen two-piece sheet metal design

The body design was developed while considering the robot's stair-climbing capabilities and fabrication efficiency. The electronics mounts inside the body will be placed symmetrically along the robot's sagittal plane to keep the center of mass as close to the center as possible, ensuring equal weight distribution across the interior. Additionally, the robot's belly thickness (i.e. the vertical distance between the hip axis and the lower body) must be minimized to maintain a higher clearance from the ground during stair climbing.

Fig. 9b shows an aluminum plate positioned in the middle, connecting the sheet metal components. However, further analysis revealed that including this plate would complicate the assembly process and introduce unnecessary stress on the screws, making it an inefficient design choice. To simplify the assembly, the final body structure will be composed of four aluminum components (two plates, two metal sheets). Lastly, the computers will be positioned distant from each other to disperse their generated heat to a wider area in the body interior to prevent the buildup of high temperatures.

Detailed Design

Legs

Each of the front legs and hind legs have 3 degrees of freedom, as shown in Fig. 10. In the hind leg, the middle and lower links are coupled together via a redundant parallel mechanism, as illustrated in Fig. 11. This three-link hind leg design was inspired by the MIT Cheetah 2 leg design, which is derived from a cheetah leg, coincidentally similar to a dog (Park). Compared to the legs of a golden retriever, our leg design simplifies the carpus (wrist) of the dog into a fixed ball, effectively removing one degree of freedom in each leg. By removing this actuated joint at the wrist, the total actuatable degrees of freedom is kept to 12, which is the number required for the robot to be compatible with our customer's custom locomotion controllers.

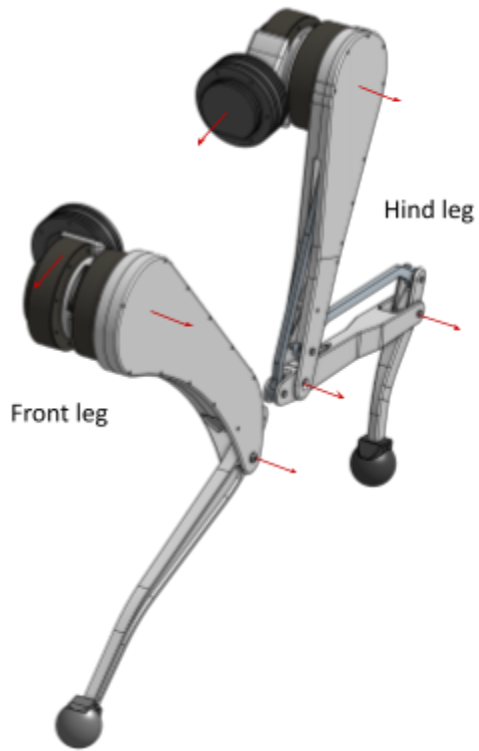


Figure 10. Joint configuration of front and hind legs. Both the front and hind legs have three degrees of freedom, where the middle link and lower link of the hind leg are coupled.

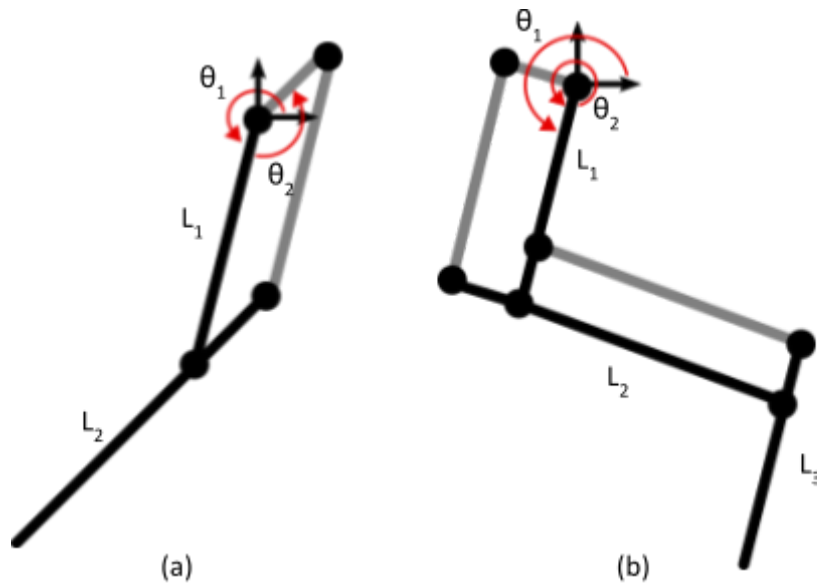


Figure 11. 2D kinematics diagrams. (a) Front leg. (b) Hind leg.

The leg lengths were optimized through a stair-climbing evaluation method developed by Barasuol (Barasuol). The details of this analysis will be covered in the Detailed Engineering Analysis section. Using the stair climbing analysis, we aimed to make the body height as short as possible to promote a lower center of gravity for stable walking, while maintaining a >30% coverage of the stair surface, which exceeds the 20% coverage requirement for stair climbing as noted by Barasuol et al. (Barasuol).

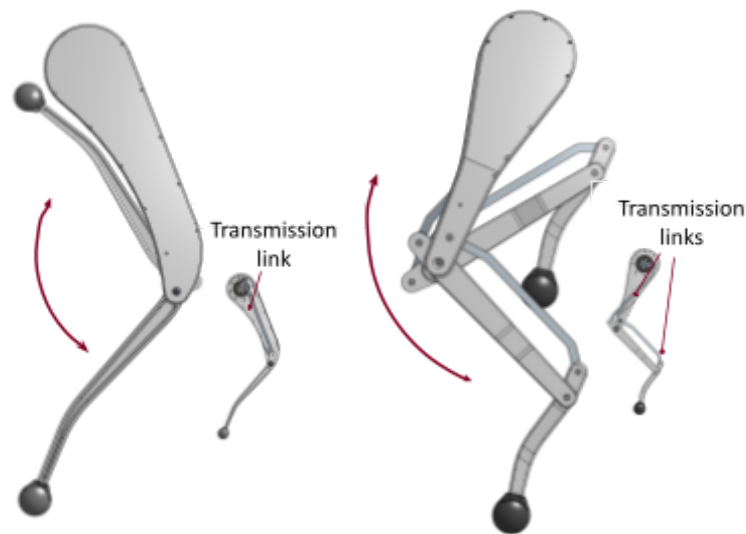


Figure 12. Leg Final Design and Actuation

For the redundant parallel transmission mechanism, a combination of radial ball bearings and steel pins were utilized at each revolute joint, which is a common design choice for many quadruped robots (Katz). Radial ball bearings were selected due to the absence of axial forces during locomotion, and ball bearings provide lower friction at the joints, reducing energy losses. The internal transmission links are modeled with AISI 1018 steel to ensure a compact frontal profile of the leg, while the linkages themselves are modeled with Aluminum 6061 to minimize the leg weight while maximizing manufacturability. Lastly, the point foot is modeled as a thermoplastic polyurethane (TPU), which can be 3D printed. This elastomer was selected as the foot material because it provides the ideal coefficient of friction, and its 3D printed structure allows easy access for manufacturing.

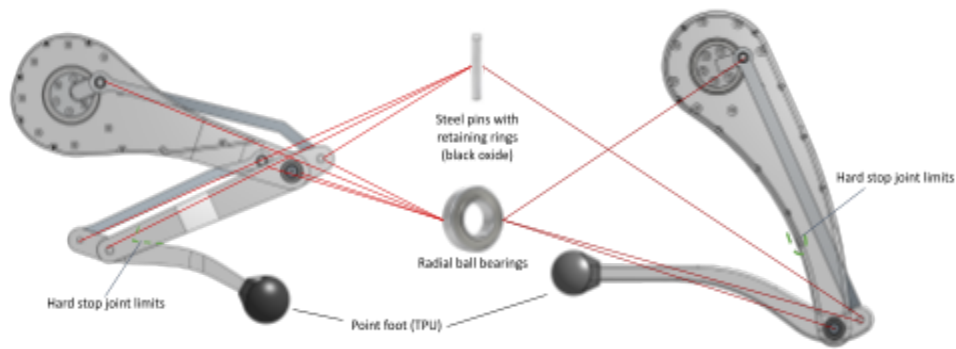


Figure 13. Internal Leg Mechanism. Transmission links (grey) are made of steel, and the linkages (white) are made with aluminum.

The cross sections for the leg designs were selected based on weight and manufacturability. It is to be noted that we plan on getting the components milled via a contract manufacturer. Based on the statics analysis presented in the Detailed Engineering Analysis section, the I-beam and square profiles were found to be the most feasible to be manufactured via milling. In the end, the square profiles were selected for their exceptional manufacturability and largest stiffness. As a safety precaution, an impact force analysis was conducted to ensure that the robot is able to withstand abrupt drops, which is detailed in the analysis section.

Body

The body design underwent several iterations to get to the final version. Aluminum was chosen as the primary material due to its combination of relatively high strength, good workability, and excellent corrosion resistance. The final dimensions of the body provide ample space to house all the electronics while maintaining a compact form factor that fits neatly into a carry-on suitcase dimensions.

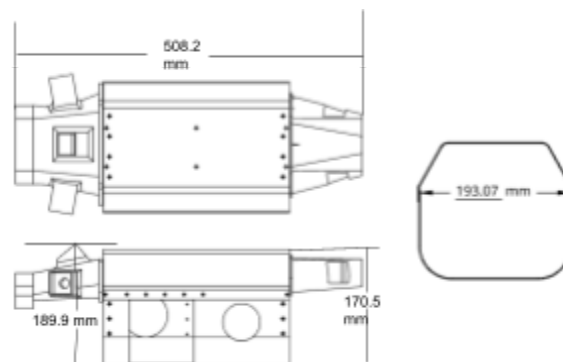


Figure 14. Body Final Dimensions

The body is constructed using two aluminum plates positioned at the front and back of the robot. These plates are encased by two pieces of sheet metal that wrap around them, overlapping at the sides and secured with screws. This design ensures a strong and durable structure while optimizing interior space for electronics placement. The components inside are arranged to prevent overheating, with the two computers mounted on opposite sides of the body. These are oriented outward to accommodate the cooling fans and improve accessibility for users.

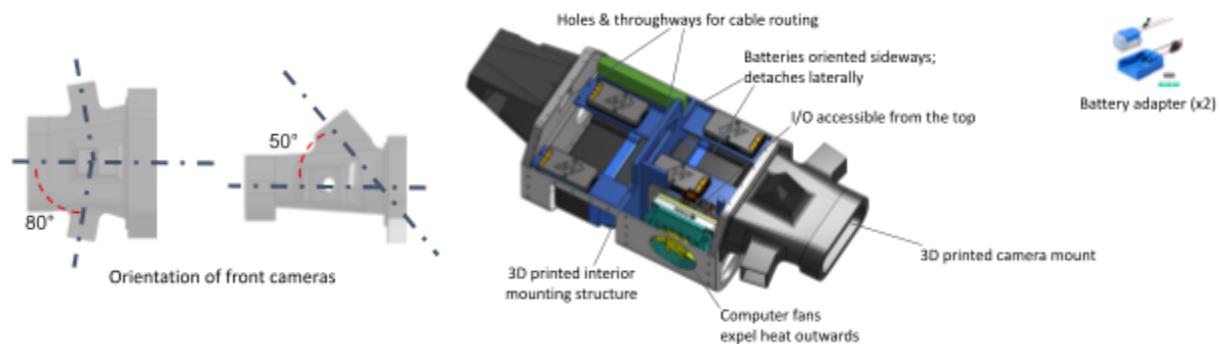


Figure 15. Internal Layout of Final Design

By hand-calculations were conducted to determine the sheet metal thickness required to minimize deflection under the weight of the electronics. A thickness of 1.5 mm was selected as it provides the necessary structural strength while remaining lightweight.

Throughout the design process, manufacturability was a key consideration. Components were designed with practical production methods in mind. For example, the overlapping metal parts on the top and bottom of the body are formed using sheet metal bending, while the aluminum plates are CNC-machined. Additional components, such as camera mounts, are 3D printed using PLA. To ensure a strong and secure assembly, M2 screws are used throughout the robot's structure.

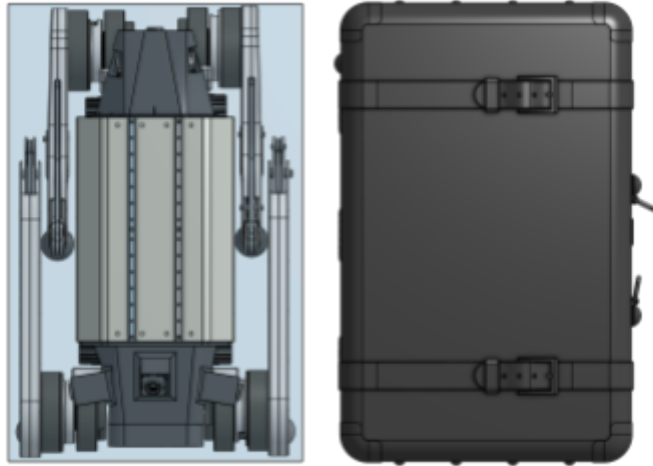


Figure 16. Vivo fits into suitcase dimensions

Feedback From Sponsors and Mentors

To validate our design and analysis, we consulted with three faculty members from the Department of Mechanical and Industrial Engineering at UMass Amherst. During our design stage, Professor Frank Sup suggested that we explore bio-inspired leg designs for maximizing locomotion efficiency, which is the design approach we utilized. Professor Govind Srimathveeravalli suggested against the use of FEA to confirm the structural integrity of our design, and instead advised us to rely solely on by-hand statics calculations. The reasoning behind this was the materials (aluminum and steel) that are used in our design can be assumed to be strong enough to withstand expected forces under a simplified beam model. Lastly, we met with Professor Yubing Sun to validate our by-hand statics analysis. Additionally, we consulted our sponsor, the Dynamic and Autonomous Robotic Systems Lab, to confirm our kinematics and dynamics models.

Cost Efficiency

3D printing technology will be utilized for the camera mounts, point feet, and internal electronics mounts for its ease of manufacturing and low cost. The use of thermoplastic polyurethane (TPU) for the point feet allows us to 3D print the feet in house, cutting costs. The electronic mounts in the body and the detachable camera mounts will be 3D printed from polylactic acid (PLA) due to its ease of access and the ability to more easily edit small features of the design in future iterations. A down selection process was used when determining the manufacturing method for the body and the legs to minimize cost while ensuring quality and structural integrity. Ultimately through this process

bending moment diagrams were created to determine the internal forces and moments within the linkages.

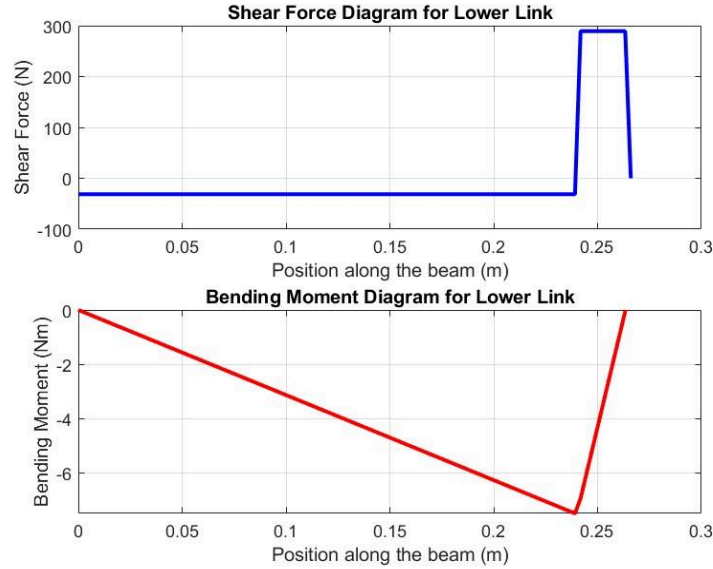


Figure 18. Shear Force and Bending Moment Diagrams for the front lower link

Fig. 18 demonstrates the shear-force and bending moment diagram for the lower link of the front leg and similar diagrams were found for all the links. When the shear-force and bending moment diagrams both go back to zero it indicates the assumptions made and the force equations found are accurate. Using the internal moment and forces of the linkages the design constraints for the cross-section were found by using the section modulus.

The section modulus stems from the cross section of a beam and is defined by,

$$S = \frac{I_z}{c}, \quad (2)$$

where I_z is the moment of inertia and c is the distance between where the maximum stress occurs and the neutral axis. The section modulus can be utilized as a constraint when creating the cross-sectional area of the link. The section modulus originates from

$$\sigma_{max} = \frac{(M_{max} \times c)}{I_z}, \quad (3)$$

where σ_{max} is the maximum allowable stress, M_{max} is the maximum bending moment. Using the bending moment diagrams the maximum moment is found while the maximum allowable stress was found by utilizing,

$$FOS = \frac{\sigma_{yield}}{\sigma_{max}} \quad (4)$$

where FOS is the the desired factor of safety and σ_{yield} is the yield strength of the material of the link link. A factor of safety of 10 was used to deter high stresses from being applied to the links. The transmission links are made of Carbon Steel 1018 while the rest of the links are made of Aluminum 6061-T6. By simplifying equation 3 the section modulus can be found using

$$S = \frac{I_z}{c} = \frac{M_{max}}{\sigma_{max}}. \quad (5)$$

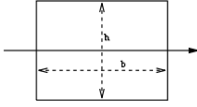
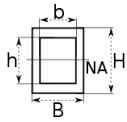
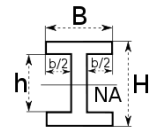
Table 5 contains the constraints for all links in both the front and hind leg in order to withstand the stresses from the maximum dynamic load.

Table 5. Design constraint for section modulus of all legs

Front Leg		Hind Leg	
Link:	Section Modulus:	Link:	Section Modulus:
Lower	$S \geq 0.31 \text{ mm}^3$	Lower	$S \geq 1.16 \text{ mm}^3$
Upper	$S \geq 3.47 \text{ mm}^3$	Middle	$S \geq 0.14 \text{ mm}^3$
Transmission	$S \geq 2.38 \text{ mm}^3$	Middle Transmission	$S \geq 1.40 \text{ mm}^3$
~	~	Upper	$S \geq 3.84 \text{ mm}^3$
~	~	Upper Transmission	$S \geq 0.60 \text{ mm}^3$

Using table 6 a cross-section can be chosen that conforms with the design constraint laid out in table 5.

Table 6. Equations to calculate section modulus for different cross sections

Shape of cross section	Section modulus equation
<p>Rectangle</p> 	$S = \frac{bh^2}{6}$
<p>Hollow rectangle</p> 	$S = \frac{BH^2}{6} - \frac{bh^3}{6H}$
<p>I-Beam</p> 	$S = \frac{BH^2}{6} - \frac{bh^3}{6H}$

Note: Adapted from “Section Modulus and Calculator Common Shape”, 2024, Engineers Edge.

In the final design concept, the rectangle was the chosen cross-section for the lower links of both legs. To provide a margin of safety, the final section modulus were set at twice their minimum required. The chosen cross-sectional dimensions are displayed in Tables 7 & 8.

Table 7. Cross-sectional dimensions for front leg links.

Leg Type	Cross Section Type	Dimensions (mm)	Section Modulus (mm ³)
Upper Link	Hollow rectangle	Inner base = 21 .00 Inner height = 41.22 Outer base = 25.00 Outer height = 46.25	3.61e+03
Lower Link	Rectangle	Base = 10.00 Height = 12.00	3.75e+02

Table 8. Cross-sectional dimensions for hind leg links.

Leg Type	Cross Section Type	Dimensions (mm)	Section Modulus (mm ³)
Upper Link	Hollow rectangle	Inner base = 18.00 Inner height = 24.00 Outer base = 24.00 Outer height = 30.00	1.87e+03
Middle Link	Rectangle	Base = 14.00 Height = 20.00	9.33
Lower Link	Rectangle	Base = 10.00 Height = 15.00	2.40e+02

Buckling Analysis

By-hand buckling analysis was conducted to evaluate the stability under compressive loads, as listed in Fig. 19. Our sponsor required us to conduct buckling analysis of the lower links, which they stated is a common failure reason for legged robots. The Euler Column buckling formula is given by

$$P_{cr} = \frac{\pi^2 EI}{L_e^3} \quad (6)$$

where P_{cr} is the critical compressive buckling force, E is the elastic modulus, I is the moment of area, and L_e is the length of the member. Using the smallest area moment of inertia of $I = 2.812 \times 10^{-9} m^4$ derived from the section modulus of the lower link in Table 7, we calculated the P_{cr} to be 74700 N, which exceeds the calculated impact force of 485.25 N. This ensures that the legs do not buckle, even under extreme conditions.

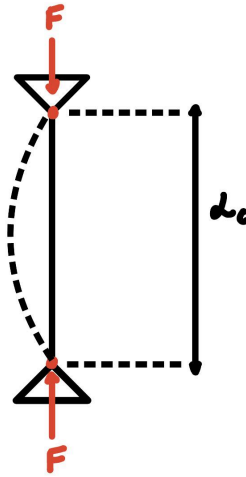


Figure 19. Euler buckling analysis diagram

Impact Force Calculation

Our robot will be traveling on planes with its owners and will be treated as carry-on luggage at times. There will come times when it is added to the carry-on cabinet of a plane and the hardware design must be able to withstand a fall at that height. The maximum height was assumed to be the height from the floor of the aircraft to the overhead cabinet height (“How Are Overhead Bins Being Modified?”).

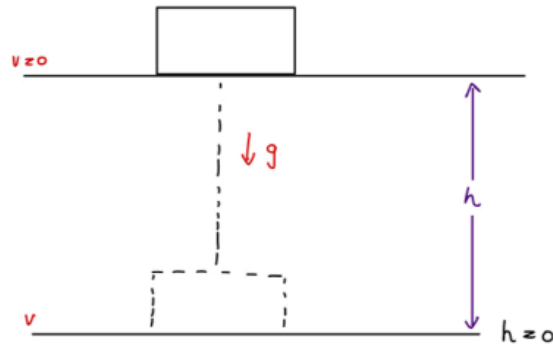


Figure 20. Diagram illustrating the free fall of the robot from the overhead cabinet of an aircraft.

Within the analysis air resistance was neglected and using energy conservation between the floor of the aircraft and height of the cabinet,

$$\text{Total potential energy of the system} = \text{Total kinetic energy of the system}$$

$$\frac{1}{2}mv_0^2 + \frac{1}{2}mv_1^2 = mgh_0 + mgh_1 \quad (7)$$

where m is the mass of the robot, g is the gravitational acceleration, v_0 is the initial velocity, v_1 is the final velocity, h_0 is the initial height and h_1 is the final height.

Since $v_0 = 0$ and $h_1 = 0$, eq (7) is simplified to,

$$v_1 = \sqrt{2gh_0} \quad (8)$$

where $g = 9.81 \text{ m/s}^2$ and $h_0 = 2.1336 \text{ m}$ (84 inches) Therefore equation (8) gives v_1 (velocity when the object hits the ground) = 6.47 m/s. Using $F = ma$, to find the impact force at collision with the ground,

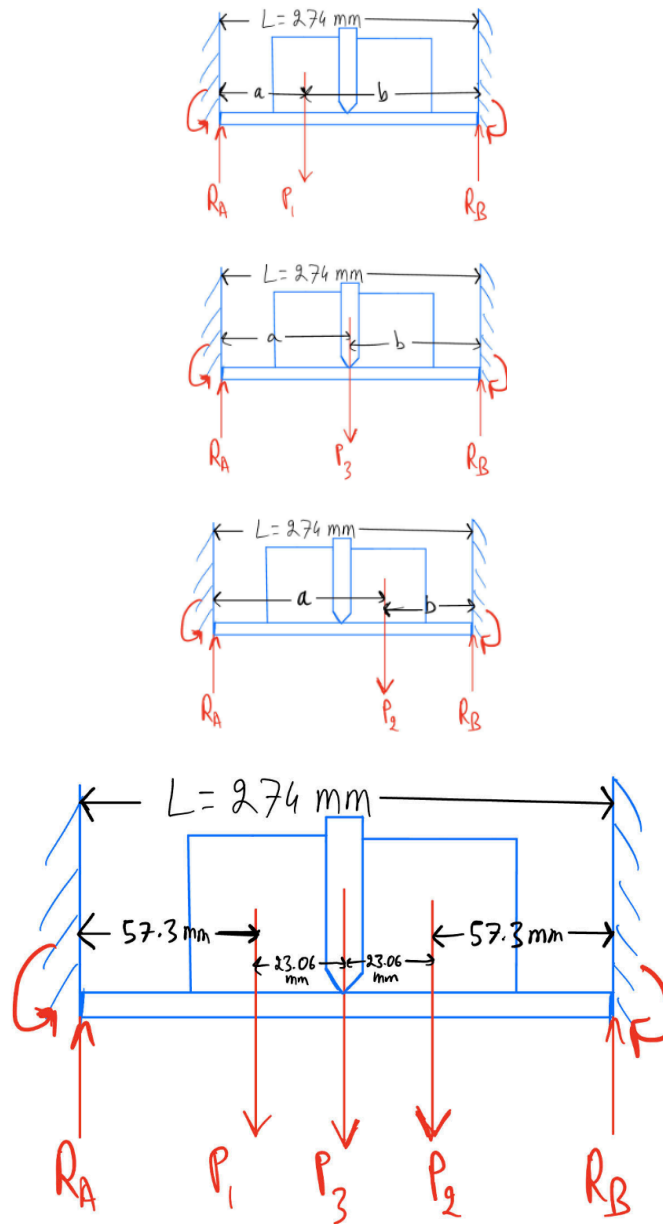
$$F = ma = \frac{m\Delta v}{\Delta t} = \frac{m(v_2 - v_1)}{\Delta t} \quad (9)$$

where F is the impact force, v_1 is the velocity when it hits the ground, v_2 is the velocity when it decelerates to stop after hitting the ground, and Δt is the time taken for the collision (time taken for the velocity to come to zero).

Assuming the time for a collision to be 200ms, considering the mass to be 15 kg (mass of the robot) and $v_2 = 0$, from equation (9), we get the impact force to be, 485.25 N.

Since the impact force is smaller than the dynamic load of the robot, we considered the dynamic load to be the maximum force the robot will have to withstand.

The bottom sheet metal, which supports the weight of the batteries and electronics, was modeled as a fixed beam. This configuration is appropriate as the sheet metal is securely screwed into an aluminum plate at both ends and in all directions, creating fixed boundary conditions.



27

The body of the robot is designed to symmetrically house all electronic components. The main heavy components considered in the analysis include:

- Two 24V 6Ah Kobalt batteries, each weighing 0.563 kg.
- A Jetson computer weighing 1.095 kg.

The Jetson computer is mounted on a PLA structure attached to the center of the body. For simplicity, we assumed that the combined weight of the Jetson computer, PLA structure, and aluminum sheet acts as a point load at the center of the beam.

Our primary objective is to evaluate the deflection of the sheet metal under these concentrated loads. Using the deflection formula for a point load on a fixed beam, we calculated the deflections at three distinct points where the loads are applied:

- P1 is the weight of battery one.
- P2 is the weight of battery two.
- P3 is the weight of PLA structure, sheet metal, and computers.

The formula of deflection at a point load is:

$$\delta = \frac{P \cdot b^3 \cdot a^3}{3EI L^3} \quad (10)$$

Figures for each load are represented on the right.

Using the method of superposition (Juvinall, 130), adding up the deflections experienced at any point load would be a quick and efficient estimation for the total deflection:

$$\delta_{total} = \delta_1 + \delta_2 + \delta_3 \quad (11)$$

Kinematic Analysis

To validate the robot's ability to climb stairs of standard height and optimize the link lengths to be as short as possible to maximize portability, an inverse kinematics analysis was conducted on each leg design using the stair climbing evaluation method developed by Barasuol et al (Barasuol). The code for this analysis is available in the GitHub repository listed in Appendix D. The inverse kinematics problem was formulated in 2D for four steps of stairs of standard height, in compliance with ADA standards ("Chapter 5: Stairways").

$$x = l_1 \cos(\theta_1) + l_2 \cos(\theta_1 + \theta_2) \quad (12)$$

$$y = l_1 \sin(\theta_1) + l_2 \sin(\theta_1 + \theta_2) \quad (13)$$

Using the forward kinematics equations, a Jacobian matrix in the world frame was derived for the inverse kinematics solver, where,

$$J = \begin{bmatrix} \frac{\partial x}{\partial \theta_1} & \frac{\partial x}{\partial \theta_2} \\ \frac{\partial y}{\partial \theta_1} & \frac{\partial y}{\partial \theta_2} \end{bmatrix} \quad (14)$$

The inverse kinematics for each leg was solved using the Newton-Raphson method to calculate the joint angles required to reach each desired footstep location (Anstee; Lynch and Park). The possible footstep locations were established by dividing the staircase by discrete points that are 1 cm apart.

The analysis is conducted as follows. Initially, the robot's dimension (belly thickness, link lengths, link thickness), are defined. Then, starting from a hip height set by the user, the inverse kinematics from the foot to each discrete point along the staircase. Any foothold position that causes the robot to reach its joint limit or penetrate the staircase are deemed as failure. Upon completion of the iterative inverse kinematics calculations of the initial hip position, the stair surface coverage, defined as the number of successful foothold positions / total number of discrete points, is calculated. A visualization of the foothold positions is shown in Fig. 23.

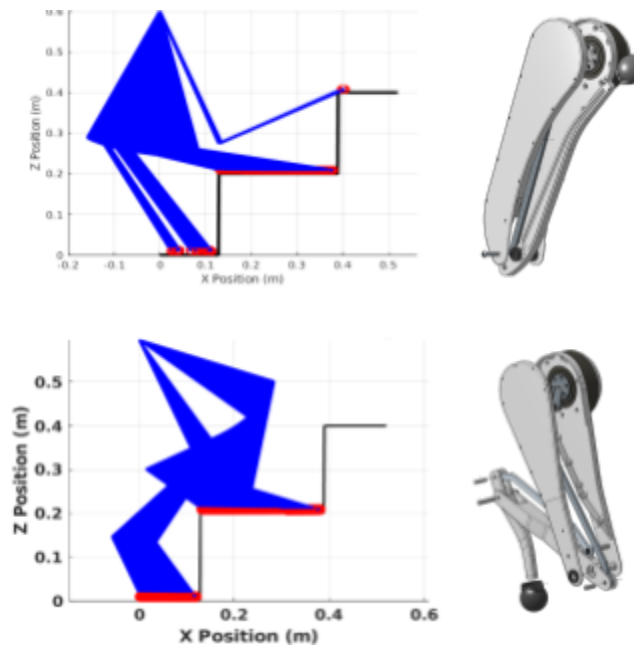


Figure 23. Kinematic visualization of front (top) and hind (bottom) legs at one hip height.

In Barasuol et al's work, leg designs capable of achieving 20% stair surface coverage were deemed to be successful at stair climbing. In our analysis, we increased this value to 30% to add a margin of safety. This increased staircase surface coverage requirement ensures that our robot has a larger workspace to promote stable stair climbing, which is crucial for a guide dog robot.

On top of validating the robot's ability to climb stairs, this analysis was used to shorten the links as much as possible to maximize portability while ensuring stair climbing. Minimization of the body height was also taken into consideration to maximize walking stability. Using a trial and error process, different combinations of link lengths and body heights were tested, arriving at a body height of 65 cm and link lengths Table 10 for the prototype design.

Table 10. Link lengths after optimization through stair climbing analysis.

	Front Leg	Hind Leg
Upper Link	300 mm	240 mm
Middle Link	-	200 mm
Lower Link	330 mm	160 mm

Dynamics Analysis

To ensure the robot is capable of generating sufficient ground reaction forces for both walking and stair climbing, a 2D inverse dynamics analysis was conducted to obtain the torque requirements of the actuators. By limiting the search space to within the expected joint angle ranges of the robot derived from the stair climbing analysis, the motor torques required to generate 75 N in the global Z direction (half of the robot's assumed weight) were calculated. The virtual work equation $\tau = J^T F_{tip}$ was utilized to find the motor torques, where $\tau \in \mathbb{R}^{2 \times 1}$ is the vector of motor torques, $J \in \mathbb{R}^{2 \times 2}$ is the Jacobian matrix in the world frame, and $F_{tip} \in \mathbb{R}^{2 \times 1}$ is the reaction force applied at the foot in the global Z direction. This method ensures the actuators are properly sized to meet the mechanical requirements of the robot's locomotion tasks while optimizing performance within the expected operational range.

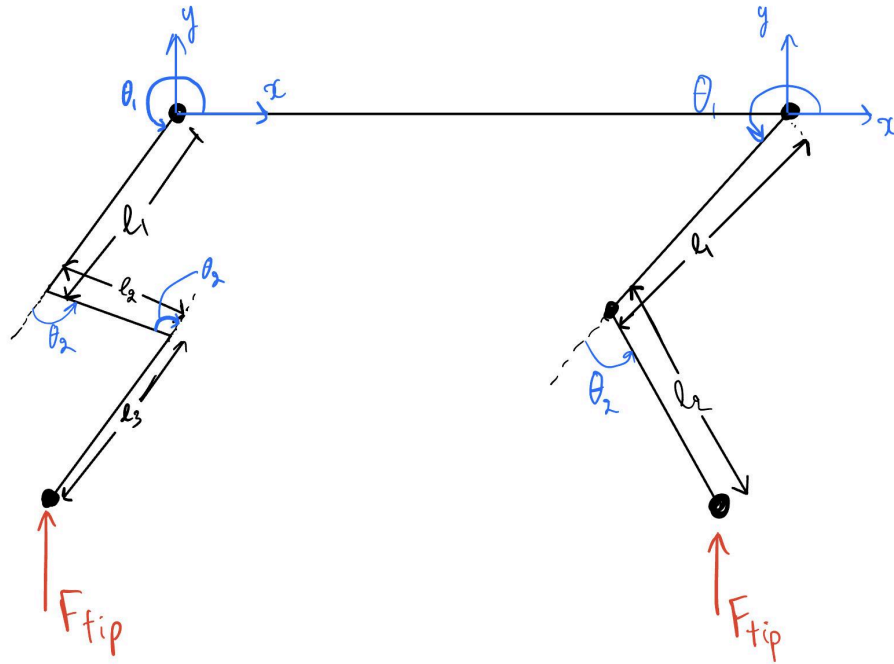


Figure 24. Free body diagram of inverse dynamics analysis, of hind leg (left) and front leg (right)

From the prototype of the CAD, the joint limit of the flexion/extension motor was found to be approximately $(20^\circ, 160^\circ)$ and $(23^\circ, 135^\circ)$ for the front and hind leg, respectively. Using these values, the maximum torque values of 17 Nm and 14 Nm were obtained from all leg designs, for the flexion/extension and abduction/adduction actuators, respectively. To streamline motor control, we

used the same motors for each type of joint. The chosen motors for flexion/extension and abduction/adduction were the T-Motor AK80-9, with a peak torque of 18 Nm, and the hip roll motors were chosen to be the T-Motor AK60-6, with a peak torque of 9 Nm. The selection of these motors was confirmed with our sponsor.

Final Design

The final concept design is presented in Fig. 27a. The bio-inspired designs imitating the anatomy of a dog are incorporated to promote locomotion efficiency. As shown in Fig. 27b, the robot is able to collapse to under carry-on suitcase dimensions.

The body is constructed with two sheet metal pieces, two CNC-machined aluminum plates, and two 3D-printed camera mounts, which support a 360-degree vision camera system. A rigid leash provided by our sponsor is securely fixed at the top of the guide dog robot, designed to enhance human-robot interaction. To further reinforce the structure, two aluminum bars are positioned at the top of the body. These bars not only add structural support but also offer additional mounting options for various components such as a microphone, and additional camera. Air cooling is incorporated into the design with computer fans oriented outward to ensure effective heat dissipation.

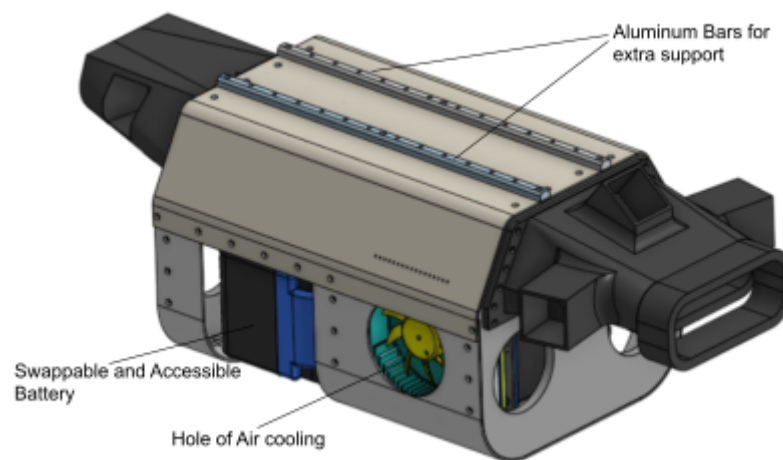


Figure 25. Isometric view of the body

The robot is powered by two 6Ah Kobalt batteries, which are designed to provide extended battery life. These batteries are both easily accessible and swappable, ensuring convenience and efficiency during operation.

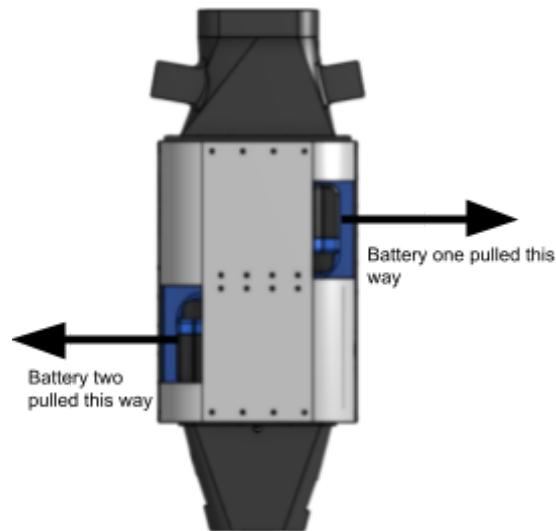


Figure 26. Body bottom view showing Battery removal

The final design of the front and hind legs both feature two degrees of freedom. The stair climbing analysis and structural analyses ensure the legs are capable of stair climbing while able to withstand large loads. The hind leg incorporates a parallel mechanism that couples the middle and lower links, inspired by the MIT Cheetah 2 leg design (Park). All metal components are designed to be manufactured by CNC milling.

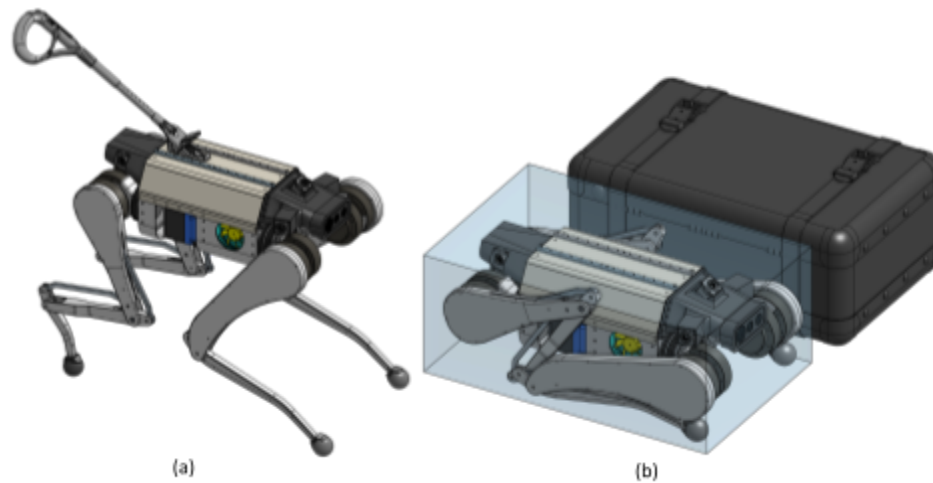


Figure 27. Final design concept. (a) Full robot assembly. (b) Comparison to carry-on suitcase size.

Design Evaluation

The evaluation process plan has been created to ensure the robot meets the design specifications...

- Evaluate whether joints move with a smooth dynamic motion
- Evaluate the ability of the robot to climb stairs and walk down hallways
- Evaluate battery life under constant use
- Measure the final weight of the assembled robot
- Check that the max temperature of CPUs meets our engineering standards (Table 2)
- Check final dimensions and verify the design meets at least marginal requirements for storability

Discussion

- Say whether marginal or ideal specifications were met or if they were not met for each specification laid out above (mass, rise/go, battery capacity, storage volume, operating temperature).
- If ideal specification was not met explain why and challenges that arised for each specification or unexpected results
- Talk about any major faults or errors, and what was learned from those mistakes
- Emphasize stair climbing more heavily and the robot dogs ability to walk in hallways and similar terrain. Talk about walking analysis done with PhD student
- Relate results back to customer requirements if necessary and customer thoughts on final results

- Any other differences between intended performance and talk about how successful the project was especially if the robot feels easily portable (lightweight)

Conclusions and Recommendations

- The guide dog was made to not only be used for research purposes, but with the potential for mass production and future iterations and electronics changes
- Covers would need to be added to back legs to prevent pinch points, though the design mostly accounts for this already (slot too small for finger for most of its length...)
- Recommendation to only make the dog so lightweight so the user can interact with the product effectively if the mass is reduced in the future
- Add further additions that could be added if more are thought of

Integrative Experience

A typical guide dog comes with heavy associated costs, responsibility, a limited timespan before retiring, and limited availability. The robot guide dog offers an excellent solution to these commonly overlooked problems that are a struggle for many BLV individuals. Our design cuts the cost of owning a guide dog in half and allows for future iterations. Though this project mainly aims to create a quadruped robot for lab research purposes, it is likely future iterations would lead to mass-production which would address not only guide dog availability but the common financial concerns and burdens that follow.

The dog was designed with the user's needs first, which has required additional research into common guide dog interactions and necessities beyond the scope of the typical engineering curriculum. Designing the legs of the robot required research into the anatomy of dogs and advanced robotics. The hind legs were designed with the ability for the user to brush their leg up against the robot, as is commonplace with traditional guide dogs. When BLV users go about their daily lives, they often need to take public transportation (Hwang). For this purpose, the dog was designed to be able to fit in a suitcase form factor and its battery increased over the sponsor's current robot. This project has gone beyond just a standard engineering design process to not simply make a barebones prototype for future iterations, but one that already addresses critical real-world problems with the current design.

Presenting our work in different ways has been an important part of this project. Tailoring our discussions to the audience allows us to inform others in a way best suited for them. Oral presentations have given us more practice in choosing the most important information to share while keeping an audience engaged. Written reports have given us the opportunity to explain in greater detail all aspects of the project, such as our preliminary research and our engineering analyses.

References

- Al Zavier, Maried. "Exploring the Use of a Drone to Guide Blind Runners." *ASSETS '16: Proceedings of the 18th International ACM SIGACCESS Conference on Computers and Accessibility*, 2016, pp. 263-264, <https://dl.acm.org/doi/abs/10.1145/2982142.2982204>.
- Anstee, Richard. "The Newton-Raphson Method." *Department of Mathematics, The University of British Columbia*, The University of British Columbia, <https://personal.math.ubc.ca/~anstee/math104/newtonmethod.pdf>.
- "ASM Material Data Sheet." *ASM Material Data Sheet*, <https://asm.matweb.com/search/specificmaterial.asp?bassnum=ma6061t6>. Accessed 8 November 2024.
- Barasuol, Victor. "Stair-Climbing Charts: On the Optimal Body Height for Quadruped Robots to Walk on Stairs." *Synergetic Cooperation Between Robots and Humans: Proceedings of the CLAWAR 2023 Conference—Volume 1*, Springer Nature Switzerland, 2024. Accessed 8 November 2024.
- Bledt, Gerardo. "MIT Cheetah 3: Design and Control of a Robust, Dynamic Quadruped Robot." *IEEE International Conference on Intelligent Robots and Systems*, 2019. *MIT Libraries*, <https://hdl.handle.net/1721.1/126619>.
- "Chapter 5: Stairways." *Access Board*, <https://www.access-board.gov/ada/guides/chapter-5-stairways/>. Accessed 5 December 2024.
- "Copper, Cu; Annealed." *MatWeb*, <https://www.matweb.com/search/DataSheet.aspx?MatGUID=9aebe83845c04c1db5126fada6f76f7e&ckck=1>.

- De Vicenti, Flavio. "Control-Aware Design Optimization for Bio-Inspired Quadruped Robots." 2021 *IEEE/RSJ International Conference on Intelligent Robots and Systems (IROS)*. International Institute of Electrical Engineers (IEEE), <https://ieeexplore.ieee.org/document/9636415>.
- Durant, A. M. "Kinematics of stair ascent in healthy dogs." *Veterinary and Comparative Orthopaedics and Traumatology*, 2011, https://www.researchgate.net/publication/49763291_Kinematics_of_stair_ascent_in_healthy_dogs.
- Guerreiro, João. "CaBot: Designing and Evaluating an Autonomous Navigation Robot for Blind People." *ASSETS '19: Proceedings of the 21st International ACM SIGACCESS Conference on Computers and Accessibility*, 2019, pp. 68-82, <https://dl.acm.org/doi/abs/10.1145/3308561.3353771>.
- "Guide Dog Class Lectures: Working in Buildings." *Guide Dogs for the Blind*, <https://www.guidedogs.com/resources/client-resources/guide-dog-class-lecture-materials/working-in-buildings>. Accessed 8 November 2024.
- "How Are Overhead Bins Being Modified?" *Rosen Aviation*, 21 February 2024, <https://www.rosenaviation.com/blog/how-are-overhead-bins-being-modified/>. Accessed 8 November 2024.
- "How Much Does A Guide Dog Cost?" *Puppy In Training*, 17 September 2017, <https://puppyintraining.com/how-much-does-a-guide-dog-cost/>.
- Hwang, Hochul. "Towards Robotic Companions: Understanding Handler-Guide Dog Interactions for Informed Guide Dog Robot Design." *CHI '24: Proceedings of the 2024 CHI Conference on Human Factors in Computing Systems*, 2024, pp. 1-20, <https://doi.org/10.1145/3613904.3642181>.

“Industrial Inspection Solutions.” *Boston Dynamics*,

<https://bostondynamics.com/solutions/inspection/>. Accessed 8 November 2024.

International Code Council, “International Residential Code. § R311.7”, 2018.

Juvinall, Robert C., and Kurt M. Marshek. *Fundamentals of Machine Component Design*. Wiley, 2019.

Katz, Benjamin G. “A low cost modular actuator for dynamic robots.” *Massachusetts Institute of Technology*, 2018, <http://hdl.handle.net/1721.1/118671>.

Layosa, Carlicia. *Timing Belt Failure and Maintenance | MISUMI Mech Lab Blog*, 15 January 2016,

<https://us.misumi-ec.com/blog/timing-belt-maintenance-and-belt-failure/>. Accessed 9 November 2024.

Lee, Jongwoo. “Energy-efficient robotic leg design using redundantly actuated parallel mechanism.”

2017 IEEE International Conference on Advanced Intelligent Mechatronics (AIM). *International Institute of Electrical Engineers (IEEE)*, <https://ieeexplore.ieee.org/document/8014182>.

Lynch, Kevin M., and Frank C. Park. *Modern Robotics: Mechanics, Planning, and Control*. Cambridge University Press, 2017.

Museum of Veterinary Anatomy FMVZ USP. *Golden Retriever dog. Canis lupus familiaris*. English:

Specimen of golden retriever skeleton prepared by the bone maceration technique and on display at the Museum of Veterinary Anatomy, FMVZ USP. 2016. *Wikimedia Commons*, https://commons.wikimedia.org/wiki/File:Golden_Retriever_dog_at_MAV-USP.jpg.

Norcross, Amanda. “Carry-on Luggage Size and Weight Limits by Airline (2024).” *U.S. News Travel*,

<https://travel.usnews.com/features/carry-on-luggage-sizes-size-restrictions-by-airline>. Accessed 8 November 2024.

Park, Hae-Won. "High-speed bounding with the MIT Cheetah 2: Control design and experiments." *The International Journal of Robotics Research*, vol. 36, no. 2, 2017. MIT Libraries, <http://hdl.handle.net/1721.1/119686>. Accessed November 2024.

Piper, Grant. "10 Guide Dog Breeds: Info, Pictures, Facts, & Traits." *Hepper Blog*, 2024, <https://www.hepper.com/guide-dog-breeds/>.

Potter, Steve D. *Screw Actuator for a Legged Robot*. US20220003297A1. United States Patent and Trademark Office, <https://patents.google.com/patent/US20220003297A1/en>.

RegulusRemains. *Unitree Go1 Calf Actuator*. <https://youtube.com/shorts/KVS0Xwg15Tc?si=qpyzFfFymUei5XW5>.

"SAE 1018 Steel – Chemical Composition, Material, Properties and Uses." *Solitaire Overseas*, <https://www.solitaire-overseas.com/blog/sae-1018-steel-composition-properties/>. Accessed 8 November 2024.

Scafato, Alessandro Schiavone. *Limb portion of robot*. WO2022207106A1. The United States Patent and Trademark Office, 2021, <https://patents.google.com/patent/WO2022207106A1/>.

Seok, Sangok. "Design Principles for Energy-Efficient Legged Locomotion and Implementation on the MIT Cheetah Robot." *IEEE/ASME Transactions on Mechatronics* 20.3 (2015), 2014, p. 1117, <http://dx.doi.org/10.1109/TMECH.2014.2339013>.

Slade, Patrick. "Multimodal sensing and intuitive steering assistance improve navigation and mobility for people with impaired vision." *Science Robotics*, vol. 6, no. 59, 2021, <https://www.science.org/doi/full/10.1126/scirobotics.abg6594>.

Standard Specification for Aluminum-Alloy 6061-T6 Standard Structural Profiles. American Society for Testing and Materials, 2010.

Tachi, Susumu. "Guide Dog Robot." *Mechanical Engineering Laboratory, Ministry of International Trade and Industry*, 1985, <https://files.tachilab.org/publications/paper1900/tachi1985MIT.pdf>.

"Thermoplastics - Physical Properties." *The Engineering ToolBox*, https://www.engineeringtoolbox.com/physical-properties-thermoplastics-d_808.html.
Accessed 8 November 2024.

"Unitree Go1." *Unitree*, <https://www.unitree.com/go1>.

APPENDIX A: Preliminary Bill of Materials for Prototype

Group 1411 Preliminary Budget, MIE 415Y (Guide Dog Robot)										
No.	Item Name	Details	Quantity	Price Per Item	Total Price (no tax)	Supplier	Part No.	URL	Funding Source	Notes
1	Deep Groove Ball Bearing	Small, Double Shielded, 440C Stainless Steel	12	\$7.92	\$95.04	MiSUMi USA	SB676 ZZ	URL	MIE	Bearings for legs
2	Precision Pivot Pins	Straight, Retaining Rings	2	\$18.45	\$36.90	MiSUMi USA	CCGH 6-14	URL	MIE	Pins for legs
3	Precision Pivot Pins	Straight, Retaining Rings	2	\$18.45	\$36.90	MiSUMi USA	CCGH 6-27	URL	MIE	Pins for legs
4	Precision Pivot Pins	Straight, Retaining Rings	2	\$18.45	\$36.90	MiSUMi USA	CCGH 6-27	URL	MIE	Pins for legs
5	Precision Pivot Pins	Straight, Retaining Rings	2	\$18.45	\$36.90	MiSUMi USA	CCGH 6-28	URL	MIE	
6	MISUMI USA estimated shipping				\$32.60	MiSUMi USA			MIE	

7	Ball Bearing	Sealed, Trade No. 6800-2RS, for 10 mm Shaft Diameter	12	\$6.63	\$79.56	McMaste r-Carr	5972K 275	URL	MIE	Bearings for legs
8	External Retaining Ring	for 6 mm OD, Black-Phosphate 1060-1090 Spring Steel	1	\$8.10	\$8.10	McMaste r-Carr	98541 A114	URL	MIE	Retaining rings for fastening pin
9	McMaster-Carr estimated shipping	Cost of shipping	1	\$10.88	\$10.88	McMaste r-Carr			MIE	
10	DURAMIC 3D TPU Filament 1.75mm Black, TPU Flexible Filament 95A, Soft TPU 3D Printing Filament, 1kg Spool, Dimensional Accuracy +/- 0.05mm, Black 1 Pack	Filament for 3D printed feet	1	\$17.00	\$17.00	Amazon		URL	MIE	3D printing material for foot
11	AK80-9 48V Robotic Dynamic	KV100	8	\$0.00	\$0.00	RobotSho p	RM-C UBE-0 08	URL	Sponsor donated	Hip pitch motors
12	AK60-6 V1.1 24V Exoskeleton Module-KV80	KV80	4	\$0.00	\$0.00	RobotSho p	RM-C UBE-0 02	URL	Sponsor donated	Hip roll motors
13	CANdle HAT		4	\$0.00	\$0.00	MAB Robotics		URL	Sponsor donated	USB to CAN bridge
14	Front Leg (aluminum 6061 + 1018 steel)		2	\$0.00	\$0.00	Contract manufact urer			Sponsor donated	
15	Hind Leg		2	\$0.00	\$0.00	Contract manufact urer			Sponsor donated	
16	Body Components		1	\$0.00	\$0.00	Contract manufact urer			Sponsor donated	
17	Kobalt 24-V Lithium Battery (6 Ah)		2	\$0.00	\$0.00	Lowes		URL	Sponsor donated	Drill batteries
18	MD80 v3.0 motor controller		12	\$0.00	\$0.00	MAB Robotics		URL	Sponsor donated	Motor controllers
19	Power board		1	\$0.00	\$0.00	JLCPCB			Sponsor donated	

					Grand Total:	\$390.78				

APPENDIX B: House of Quality

X	Negative Influence
✓	Positive Influence

"+" Positive Relationship
0 - Average relationship
"-" Minimum Relationship

Customer Attributes, Needs, Requirements, or Demanded Quality	Relative Weight	Engineering Metrics or Requirements					Now			
		Battery Capacity	Weight	Storage Volume	Reachable Workspace (rise/go)	Operating Temperature	My Product	Spot (Boston Dynamics)	Go1 (Unitree)	Aliengo (Unitree)
Storability/Small Size	4	+	+	+	0		5	0	5	1
Temperature Control	2	0				+	3	5	3	4
Operating Time	5	+	+			0	3	3	2	5
Portability	3	0	+	0	0		5	1	5	4
Cost	1	+		-	-		4	1	5	2
Hardware For Stair Climbing	6		+	0	+		4	5	2	4
Direction of Improvement		↑	↓	↓	↑	↓				
Measurement Units		W*h	kg	m³	m/m	°C				
Spot (Boston Dynamics)		564	33.8	1	0.32/ 0.35	55				
Go1 (Unitree)		133.2	12	.02	0.12/ 0.27	-				
AlienGo (Unitree)		317.1	19	0.03	0.32/ 0.35	-				
Ideal Target Specification Values		288	≤ 21.5	< 0.454	0.20/ 0.25	< 55				
Marginal Target Specification Values		134	≤ 25	0.454	0.18/ 0.28	55				

APPENDIX C: Battery Calculations

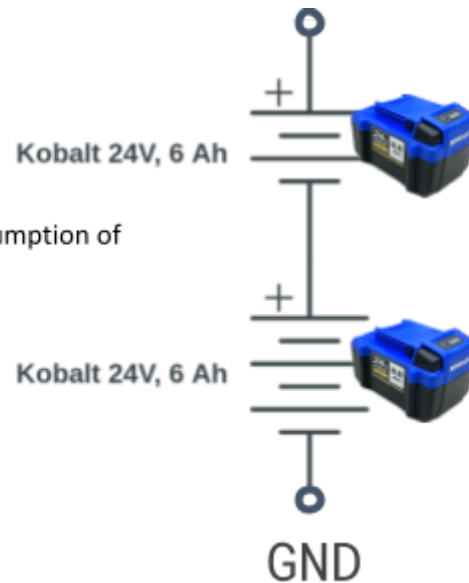
$V = 24 [V]$ battery voltage

$C = 6 [Ah]$ battery capacity

$P_{consumed} \approx 400 [W]$ estimated power consumption of ANYmal robot (Hutter)

$$T = \frac{2 \cdot V \cdot C [Whr]}{P [W]} = \frac{2 \cdot 24 \cdot 6}{400} [hr]$$

$T = 0.72 [hr]$ battery life



APPENDIX D: Stair Climbing Analysis & Inverse Dynamics Code Repositories

[Stair Climbing Analysis Script](#)

[Inverse Dynamics Analysis Scripts](#)